

# Pd Uptake and H<sub>2</sub>S Sensing by an Amphoteric Metal–Organic Framework with a Soft Core and Rigid Side Arms\*\*

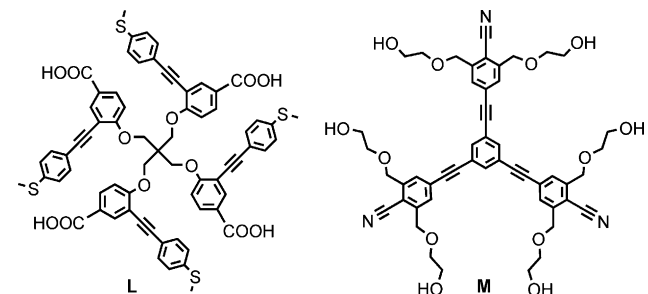
Jieshun Cui, Yan-Lung Wong, Matthias Zeller, Allen D. Hunter, and Zhengtao Xu\*

**Abstract:** Molecular components of opposite character are often incorporated within a single system, with a rigid core and flexible side arms being a common design choice. Herein, molecule L has been designed and prepared featuring the reverse design, with rigid side arms (arylalkynyl) serving to calibrate the mobility of the flexible polyether links in the core. Crystallization of this molecule with Pb<sup>II</sup> ions led to a dynamic metal–organic framework (MOF) system that not only exhibits dramatic, reversible single-crystal-to-single-crystal transformations, but combines distinct donor and acceptor characteristics, allowing for substantial uptake of PdCl<sub>2</sub> and colorimetric sensing of H<sub>2</sub>S in water.

As in many domains in the arts and sciences, the integration and interplay of opposing characters is a common thread in chemistry. This interplay is reflected in the classical systems of liquid crystals (with rigid and floppy components), surfactants (hydrophilic/hydrophobic components), and semiconductors (holes/electrons). More recent reports in this vein include frustrated Lewis acid–base pairs for H<sub>2</sub> activation<sup>[1]</sup> and ditopic receptors<sup>[2]</sup> for simultaneous anion and cation binding (ion-pair recognition). In the growing field of metal–organic frameworks,<sup>[3]</sup> this incorporation of components of opposite character manifests itself in the combination of hard and soft groups (e.g., carboxylate and sulfur/nitrogen donors),<sup>[4]</sup> and in various floppy side chains tethered to rigid backbones.<sup>[5]</sup> Such reports on bifunctional MOF systems generally aim to exploit the tunable porous properties of MOFs to enhance the guest-binding properties for applications including separation,<sup>[5d,6]</sup> sensing,<sup>[4d,7]</sup> and catalysis.<sup>[6c,8]</sup> For example, thioether/thiol groups affixed to carboxylate building blocks tend to remain freestanding in frameworks formed with hard metal ions (Zr<sup>IV</sup>, Al<sup>III</sup>, Cr<sup>III</sup>, Eu<sup>III</sup>), and thereby facilitate the uptake of (soft) metal species.<sup>[4a–c]</sup> These donor-equipped MOF systems complement systems that feature open metal sites<sup>[9]</sup> as

acceptors for binding Lewis bases as guests. Prompted by the appeal of this concept as well as the potentially rich host–guest chemistry, we aimed to achieve the formation of a MOF system that simultaneously combines distinct donor and acceptor characteristics, a topic that, to our knowledge, has not yet been addressed.

Herein, we report that backfolded molecule L (Scheme 1) and Pb<sup>II</sup> ions form a flexible framework that represents a step towards our goal. This system displays distinct amphoteric behavior, facilitated by the coexistence of free-standing sulfur



**Scheme 1.** Backfolded molecule L and compound M with the “starburst” form of a traditional dendrimer. The rigid phenylacetylene (green) components act as the side chains in L but as the backbone in M.

(and the alkyne and ether) donors and labile capped Pb<sup>II</sup> centers as accessible acceptor sites, which manifests itself in the effective uptake of both Lewis acid (such as PdCl<sub>2</sub>) and Lewis base (such as H<sub>2</sub>S) guests. Notwithstanding the serendipitous nature of this discovery, molecule L is composed of design elements that both follow and break from previous works. First, the design carries over from the hard and soft components strategy, as seen in the hard carboxy (as the primary donors for framework formation) and soft donors on the side arms. Also the side arms are backfolded, pointing away from the carboxy groups, in contrast with the “starburst” form of a traditional dendrimer (see Scheme 1 for example). The backfolded configuration has been explored for network construction;<sup>[10]</sup> in the present case, it serves to minimize direct steric/chemical influence on the carboxy groups.

Most notable, however, is the configuration of the rigid side arms (the phenylacetylene component) and the flexible backbone (the pentaerythritol ether hinges)<sup>[11]</sup> in L, which reverses the conventional design of flexible side arms attached to rigid backbones (see molecule M in Scheme 1 as an early example<sup>[5b]</sup>). In particular, rigid units are widely integrated as the linker backbone<sup>[12]</sup> because the shape persistence and directionality often lead to networks of robust pores and regular topologies. Herein, we place the

[\*] J. Cui, Y.-L. Wong, Dr. Z. Xu

Department of Biology and Chemistry

City University of Hong Kong

83 Tat Chee Avenue, Kowloon, Hong Kong (China)

E-mail: zhengtao@cityu.edu.hk

Dr. M. Zeller, Dr. A. D. Hunter

Department of Chemistry, Youngstown State University

One University Plaza, Youngstown, OH 44555 (USA)

[\*\*] This work is supported by City University of Hong Kong (Project no. 9667092) and the Research Grants Council of HKSAR (GRF 103413). The diffractometer was funded by NSF Grant 0087210, by Ohio Board of Regents Grant CAP-491, and by Youngstown State University.

Supporting information for this article is available on the WWW under <http://dx.doi.org/10.1002/anie.201408453>.

rigid arylethynyl units in the side arms instead. By so doing, we hope to achieve systematic control over the degree of flexibility of the core unit, that is, bulky and stiff side arms would limit the motion of the core unit, imposing structural rigidity on the individual building blocks as well as the overall network.

The synthesis of L is based on well-established procedures (see Scheme S1 in the Supporting Information). The efficient Sonogashira coupling readily allows various alkynyl side arms to be attached, thus facilitating the preparation of a versatile linker system of tunable rigidity and functionality. Single crystals of the framework BFMOF-1 (BF denotes back-folded) suitable for X-ray diffraction studies were obtained by solvothermal reaction between L and  $\text{Pb}(\text{NO}_3)_2$  in a DMA/ $\text{H}_2\text{O}$  mixture of solvents (DMA = *N,N*-dimethylacetamide; detailed procedure given in the Supporting Information). Elemental and thermogravimetric analyses (Figure S1) indicates a composition of  $\text{Pb}_6\text{O}_2(\text{C}_{69}\text{H}_{48}\text{O}_{12}\text{S}_4)_2(\text{DMA})_3(\text{H}_2\text{O})_2$  for the as-prepared sample.

The proposed composition of the sample is also consistent with the X-ray crystal structure of BFMOF-1 (Figures 1 a and 2 a).<sup>[13]</sup> The crystal structure adopts the space group  $P\bar{1}$ , and features the centrosymmetric  $\text{Pb}_6\text{O}_2(\text{CO}_2)_8$  cluster (Figure 1),<sup>[14]</sup> with the two edge-sharing  $\text{Pb}_4\text{O}$  tetrahedra exhibiting short Pb–O bond lengths (i.e., 2.229, 2.251, 2.310, and 2.325 Å). By comparison, the Pb–O distances from the carboxy (-CO<sub>2</sub>) groups are longer, and vary more (for example, from 2.401, 2.512, 2.620, and 2.714 Å up to 2.981 and 3.065 Å), indicating a weaker and more reversible nature

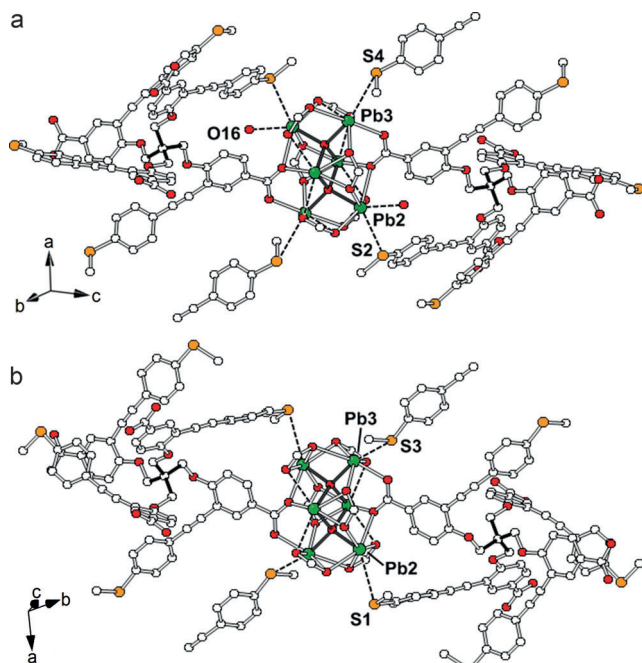


**Figure 1.** Crystal structures showing the local bonding environments of the  $\text{Pb}_6\text{O}_2$  units in a) BFMOF-1 and b) BFMOF-1 a. For each structure, two of the eight associated L molecules are displayed in full. O16 in (a) is from the bound  $\text{H}_2\text{O}$  ( $\text{Pb}–\text{O} = 2.981 \text{ \AA}$ ). Dashed lines denote  $\text{Pb}–\text{O}$  contacts greater than 2.90 Å and  $\text{Pb}–\text{S}$  contacts: a)  $\text{Pb}2–\text{S}2 = 3.329 \text{ \AA}$ ,  $\text{Pb}3–\text{S}4 = 3.954 \text{ \AA}$ ; b)  $\text{Pb}3–\text{S}3 = 3.608 \text{ \AA}$ ,  $\text{Pb}2–\text{S}1 = 3.646 \text{ \AA}$ . Atom colors: green = Pb; red = O; yellow = S; gray = C.

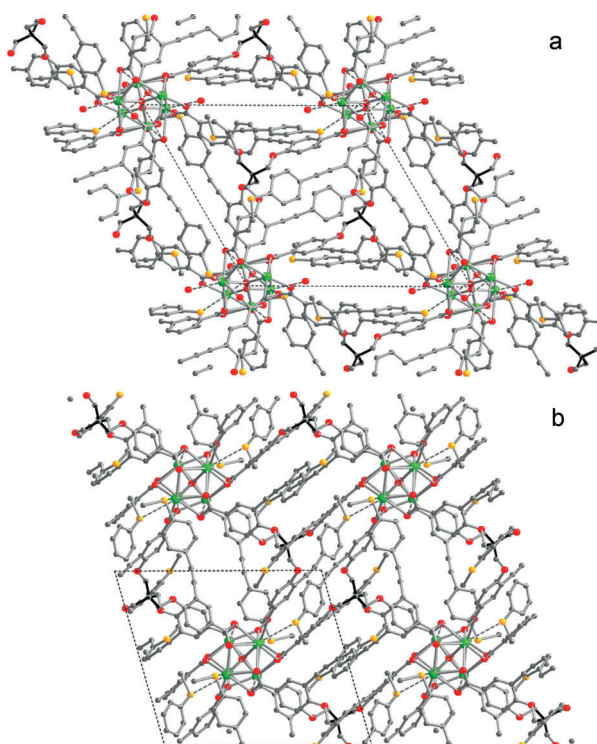


**Figure 2.** The crystal-packing structures of a) BFMOF-1 and b) BFMOF-1 a, both shown along the  $a$  axis. The DMA guests are not shown in (a). Atom colors: green = Pb; red = O; yellow = S; gray = C.

of the individual links. The asymmetric unit of the cell consists of  $(\text{Pb}_3\text{O})\text{L}(\text{H}_2\text{O})\cdot 1.5\text{DMA}$ , with the  $\text{H}_2\text{O}$  being bound by a Pb atom and the DMA molecules located in the voids. Two of the  $\text{Pb}^{II}$  centers are weakly capped by two S atoms from the side arms of L (distances: 3.329 and 3.954 Å, respectively), whereas the third Pb center is not capped—it appears to be more open. The weakly bound and open Pb centers together point to potential accessibility to guest donors. The other two S atoms of the L molecule are not coordinated to the  $\text{Pb}^{II}$  centers. As free-standing donors, they coexist with the potentially accessible  $\text{Pb}^{II}$  centers, and suggest an amphoteric character for the host network.

The BFMOF-1 grid can be viewed as a (4,8)-connected net, with the L molecule and the Pb block being 4- and 8-connected, respectively (Figure S2). The topology is that of a distorted fluorite net (comparable to that of a Zr-based MOF<sup>[15]</sup>). This net can also be dissected as two diamondoid (cubic ZnS) subnets fused at one set of the tetrahedral nodes.

When the as-prepared BFMOF-1 crystals were immersed in ethanol (or other solvents, such as  $\text{CH}_3\text{CN}$  and  $\text{CH}_2\text{Cl}_2$ ), the DMA guests were readily replaced. The resultant crystals, upon exposure to air, quickly (i.e. within 30 minutes) transform into a new crystalline phase (such as BFMOF-1 a). The quality of the X-ray crystal structure<sup>[16]</sup> for BFMOF-1 a is somewhat poorer (for example with large residual electron-density peaks near the Pb ions), which is likely caused by the structural irregularities arising from the drastic transformation in the solid state. Nonetheless, the X-ray data clearly indicate the retention of  $\text{Pb}_6\text{O}_2(\text{CO}_2)_8$  cluster (but without the associated  $\text{H}_2\text{O}$ ) and the overall fluorite topology (Figure 1 b

and 2 b). The unit cell parameters are, however, significantly changed, with a shrinkage of the cell volume (by 12%) from  $3746.8(8)$  Å<sup>3</sup> in BFMOF-1 to  $3306.5(19)$  Å<sup>3</sup> in BFMOF-1a. The daughter phase BFMOF-1a is therefore less open, and the fluoride net (Figure S2) is more distorted as compared with the parent BFMOF-1. The crystal structure of BFMOF-1a contains no DMA molecules, as is also verified by thermogravimetric analysis (Figure S1) and FTIR spectroscopy studies (Figure S3). The BFMOF-1a solid is stable in air for months, as shown by powder X-ray diffraction (PXRD; see pattern d in Figure 3).

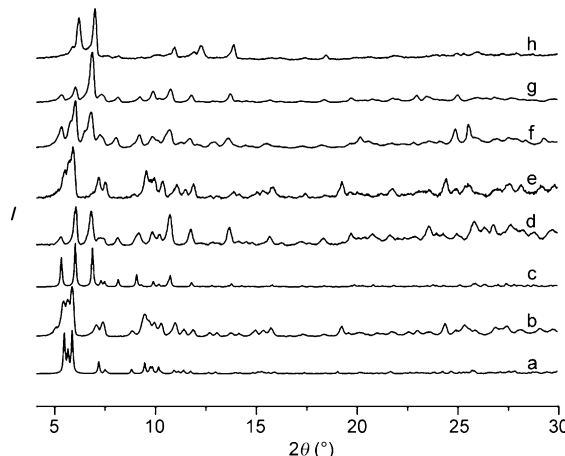


**Figure 3.** Powder X-ray diffraction patterns of BFMOF-1-related systems: a) calculated diffraction pattern from the single-crystal structure of BFMOF-1; b) an as-prepared sample of BFMOF-1; c) pattern calculated from the single-crystal structure of BFMOF-1a (the desolvated sample); d) BFMOF-1a; e) BFMOF-1a (BFMOF-1a after being heated in DMA at 120°C for 12 h); f) 1a-PdCl<sub>2</sub>; g) 1a-Pd-H<sub>2</sub>; h) 1a-H<sub>2</sub>S.

The solid sample of the desolvated phase of BFMOF-1a shows no significant N<sub>2</sub> sorption at 77 K. However, effective CO<sub>2</sub> uptake was measured at 273 K, as is shown in the highly reproducible typical type-I gas adsorption isotherms (Figure S4). The corresponding surface area is found to be  $318\text{ m}^2\text{ g}^{-1}$ , with pore volume being  $0.107\text{ ccg}^{-1}$ . The gas sorption studies therefore indicate that dynamic, cooperative diffusion processes can be achieved at higher temperatures (e.g., 273 K),<sup>[3k,17]</sup> which can be attributed to the structural flexibility built into the semirigid backbone of linker L. Additionally, BFMOF-1a can be converted back into the parent BFMOF-1 after being heated in DMA (pattern e in Figure 3; the FTIR spectrum is given in Figure S3), illustrating further the dynamics and resilience of the host net.

The Lewis base character of the BFMOF-1a net was first shown through interaction of the compound with PdCl<sub>2</sub>. Upon contact with a solution of [PdCl<sub>2</sub>(CH<sub>3</sub>CN)<sub>2</sub>] in CH<sub>2</sub>Cl<sub>2</sub>, the slightly yellow crystals of BFMOF-1a turn brownish red, with the color darkening over time (Figure S5 and S6). Inductively coupled plasma (ICP) elemental analysis indicates a Pd:Pb ratio of 2.51:1 for the PdCl<sub>2</sub>-loaded sample (1a-PdCl<sub>2</sub>; composition = Pb<sub>6</sub>O<sub>2</sub>(L)<sub>2</sub>(PdCl<sub>2</sub>)<sub>15</sub>). PXRD indicates that the original lattice of BFMOF-1a (pattern f in Figure 3) is retained but with a distinct intensity change as a result of

the additional electron density from the heavy PdCl<sub>2</sub> species. Qualitatively, the dark color can be ascribed to charge transfer from the highest occupied molecular orbitals (HOMOs) of L to the lowest unoccupied molecular orbitals (LUMOs) of PdCl<sub>2</sub>. The ether and thioether donors of L, together with the low-lying 4d orbitals of the Pd<sup>II</sup> center, apparently favor such interactions. Under similar conditions, AgBF<sub>4</sub> molecules also diffuse readily into the BFMOF-1a matrix (with an overall Ag:Pd ratio of 1.40:1, see the Supporting Information), producing a brown color. However, this brown color is lighter than that of the PdCl<sub>2</sub>-loaded sample (Figure S7). Further tests indicated a lower uptake for HgCl<sub>2</sub>, [PtCl<sub>2</sub>(CH<sub>3</sub>CN)<sub>2</sub>], and CdCl<sub>2</sub>, with the number of moles of the adsorbed Hg, Pt, or Cd ions being less than half of that of Pb (see Supporting Information), and the BFMOF-1a host remaining strongly emissive (Figure S7). We suspect that the uptake of Pd<sup>II</sup> and Ag<sup>I</sup> salts was facilitated by π-complexation with the alkyne units on the host net, whereas such interactions might be weaker for Hg<sup>II</sup> and Cd<sup>II</sup> ions.<sup>[18]</sup> As for Pt<sup>II</sup>, its very low lability likely hinders the uptake.

Upon being placed in a H<sub>2</sub> atmosphere, the crystals of 1a-PdCl<sub>2</sub> become gray, steadily turning into black within one hour (Figure S5 and S6). This color change is consistent with the reduction of the embedded Pd<sup>II</sup> ions into Pd<sup>0</sup> species. Moreover, the PXRD pattern of the H<sub>2</sub>-treated sample (that is, 1a-Pd-H<sub>2</sub>) indicates retention of the crystalline order, with no peaks corresponding to Pd particles or other crystalline impurities detected (pattern g, Figure 3). Scanning electron microscopy (Figure S8) images of the BFMOF-1a, 1a-PdCl<sub>2</sub>, and 1a-Pd-H<sub>2</sub> solids indicate similar morphologies (that is, with no extra particles present on the surface of the crystals of 1a-Pd-H<sub>2</sub>), further supporting that the Pd<sup>0</sup> species remain embedded within the host net. Compound 1a-Pd-H<sub>2</sub> will be studied as a heterogeneous catalyst, for example in hydrogenation reactions.

The Lewis acid character of BFMOF-1a was revealed in its interaction with H<sub>2</sub>S (to form 1a-H<sub>2</sub>S). Upon exposure to H<sub>2</sub>S gas, the yellowish crystals of BFMOF-1a become dark red (Figure S9), with the bluish white emission (see the spectra in Figure S10) being effectively suppressed. X-ray photoelectron spectroscopy (XPS; Figure S11) studies indicate a clear shift of the peaks attributed to Pb 4f<sub>7/2</sub> and 4f<sub>5/2</sub> states toward lower energies after H<sub>2</sub>S treatment. The dark color and the shift of the peak in the XPS spectrum are consistent with the binding of H<sub>2</sub>S species as a strong electron donor onto the Pb centers. Elemental analyses (see Supporting Information for the data) also indicate an increase of the S content, with the composition of 1a-H<sub>2</sub>S found to be Pb<sub>6</sub>O<sub>2</sub>(L)<sub>2</sub>(H<sub>2</sub>S)<sub>2</sub>(H<sub>2</sub>O)<sub>4</sub>. Each Pb<sub>6</sub>O<sub>2</sub> cluster thus appears to associate with two H<sub>2</sub>S molecules: the well-defined Pb<sub>6</sub>O<sub>2</sub>/H<sub>2</sub>S ratio indicates that the interaction with H<sub>2</sub>S is regulated within the BFMOF-1a matrix: e.g., the capping thioether S atoms on the Pb centers might serve to limit the uptake capacity under these conditions. The 1a-H<sub>2</sub>S crystals remain transparent (no cracking), with well-defined, sharp PXRD peaks (pattern h, Figure 3) indicating a highly crystalline phase. The peaks were, however, shifted to slightly higher angles compared with those of BFMOF-1a, suggesting further compaction of the host lattice after H<sub>2</sub>S treatment.

Single-crystal X-ray diffraction studies are underway to further study the structure of 1a-H<sub>2</sub>S.

The distinct color changes of the BFMOF-1 a crystals in response to H<sub>2</sub>S binding point to potential sensing applications. For example, the readily available single crystals of BFMOF-1 a provide a convenient and effective platform for sensing and quantifying purposes as a disposable sensor for H<sub>2</sub>S species. Moreover, the BFMOF-1 a solid is insoluble (whereas the commonly used lead acetate is soluble) in water and is readily applicable in monitoring H<sub>2</sub>S in water-based biological and environmental assays.<sup>[19]</sup> For example, a light but distinct red color (Figure 4) quickly developed even when H<sub>2</sub>S was present only at 17.6 μM (0.60 ppm). At the higher concentrations of 35.2 μM (1.2 ppm), 88 μM (3.0 ppm), and 352 μM (12 ppm), the color darkens systematically, indicating the potential for colorimetric analysis.

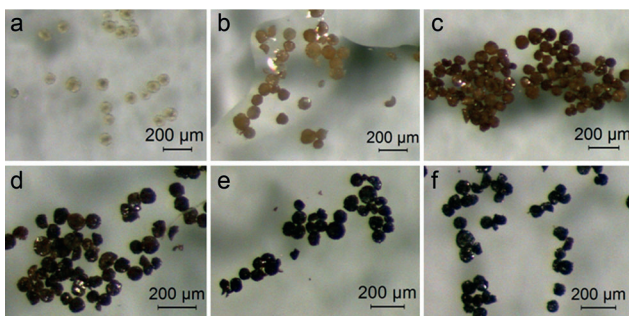


**Figure 4.** Photographs of the BFMOF-1 crystallites stirred for 0.5 hours at 80°C in solutions with H<sub>2</sub>S at various concentrations: a) 0 ppm; b) 0.6 ppm; c) 1.2 ppm; d) 3.0 ppm; e) 12 ppm and f) 60 ppm.

In conclusion, an amphoteric metal–organic framework has been characterized, with the donor and acceptor properties demonstrated in the uptake of metal salts (for example PdCl<sub>2</sub>) and H<sub>2</sub>S molecules, respectively. This material is composed of a backfolded linker unit which has a soft core and rigid arms, a feature that gives rise to the distinct framework dynamics found. Rigid side arms and the backfolded shape therefore appear to be linker features of interest in the study of other frameworks.

Received: August 22, 2014

Revised: October 9, 2014

Published online: ■■■■■

**Keywords:** donor–acceptor systems · host–guest systems · metal–organic frameworks · metal uptake · sensors

- [1] a) S. R. Flynn, D. F. Wass, *ACS Catal.* **2013**, *3*, 2574–2581; b) G. C. Welch, R. R. S. Juan, J. D. Masuda, D. W. Stephan, *Science* **2006**, *314*, 1124–1126.
- [2] a) A. J. McConnell, P. D. Beer, *Angew. Chem. Int. Ed.* **2012**, *51*, 5052–5061; *Angew. Chem.* **2012**, *124*, 5138–5148; b) S. K. Kim, G. I. Vargas-Zuniga, B. P. Hay, N. J. Young, L. H. Delmau, C. Masselin, C.-H. Lee, J. S. Kim, V. M. Lynch, B. A. Moyer, J. L. Sessler, *J. Am. Chem. Soc.* **2012**, *134*, 1782–1792; c) S.-K. Kim, J. L. Sessler, *Chem. Soc. Rev.* **2010**, *39*, 3784–3809; d) J. M.

Mahoney, A. M. Beatty, B. D. Smith, *J. Am. Chem. Soc.* **2001**, *123*, 5847–5848.

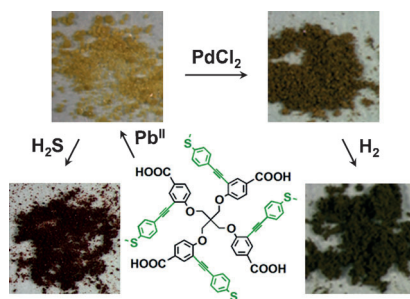
- [3] a) Y. Yan, S. Yang, A. J. Blake, M. Schröder, *Acc. Chem. Res.* **2014**, *47*, 296–307; b) S. M. Cohen, *Chem. Rev.* **2012**, *112*, 970–1000; c) W. L. Leong, J. J. Vittal, *Chem. Rev.* **2011**, *111*, 688–764; d) S. T. Meek, J. A. Greathouse, M. D. Allendorf, *Adv. Mater.* **2011**, *23*, 249–267; e) O. Shekhah, J. Liu, R. A. Fischer, C. Wöll, *Chem. Soc. Rev.* **2011**, *40*, 1081–1106; f) D. Zhao, D. J. Timmons, D. Yuan, H.-C. Zhou, *Acc. Chem. Res.* **2011**, *44*, 123–133; g) M. H. Mir, L. L. Koh, G. K. Tan, J. J. Vittal, *Angew. Chem. Int. Ed.* **2010**, *49*, 390–393; *Angew. Chem.* **2010**, *122*, 400–403; h) G. Férey, *Chem. Soc. Rev.* **2008**, *37*, 191–214; i) S. Kitagawa, R. Matsuda, *Coord. Chem. Rev.* **2007**, *251*, 2490–2509; j) Z. Xu, *Coord. Chem. Rev.* **2006**, *250*, 2745–2757; k) D. Bradshaw, J. B. Claridge, E. J. Cussen, T. J. Prior, M. J. Rosseinsky, *Acc. Chem. Res.* **2005**, *38*, 273–282; l) S. Lee, A. B. Mallik, Z. Xu, E. B. Lobkovsky, L. Tran, *Acc. Chem. Res.* **2005**, *38*, 251–261; m) N. W. Ockwig, O. Delgado-Friedrichs, M. O’Keeffe, O. M. Yaghi, *Acc. Chem. Res.* **2005**, *38*, 176–182; n) K. S. Suslick, P. Bhyrappa, J. H. Chou, M. E. Kosal, S. Nakagaki, D. W. Smith, S. R. Wilson, *Acc. Chem. Res.* **2005**, *38*, 283–291; o) O. M. Yaghi, G. M. Li, H. L. Li, *Nature* **1995**, *378*, 703–706; p) G. B. Gardner, D. Venkataraman, J. S. Moore, S. Lee, *Nature* **1995**, *374*, 792–795; q) L. R. MacGillivray, S. Subramanian, M. J. Zaworotko, *J. Chem. Soc. Chem. Commun.* **1994**, 1325–1326; r) B. H. Hoskins, R. Robson, *J. Am. Chem. Soc.* **1989**, *111*, 5962–5964; s) C. Wang, D. Liu, W. Lin, *J. Am. Chem. Soc.* **2013**, *135*, 13222–13234.
- [4] a) K.-K. Yee, N. Reimer, J. Liu, S.-Y. Cheng, S.-M. Yiu, J. Weber, N. Stock, Z. Xu, *J. Am. Chem. Soc.* **2013**, *135*, 7795–7798; b) J. He, K.-K. Yee, Z. Xu, M. Zeller, A. D. Hunter, S. S.-Y. Chui, C.-M. Che, *Chem. Mater.* **2011**, *23*, 2940–2947; c) X.-P. Zhou, Z. Xu, M. Zeller, A. D. Hunter, *Chem. Commun.* **2009**, 5439–5441; d) J. He, M. Zha, J. Cui, M. Zeller, A. D. Hunter, S.-M. Yiu, S.-T. Lee, Z. Xu, *J. Am. Chem. Soc.* **2013**, *135*, 7807–7810; e) J. He, M. Zeller, A. D. Hunter, Z. Xu, *J. Am. Chem. Soc.* **2012**, *134*, 1553–1559; f) X.-P. Zhou, Z. Xu, J. He, M. Zeller, A. D. Hunter, R. Clérac, C. Mathonière, S. S.-Y. Chui, C.-M. Che, *Inorg. Chem.* **2010**, *49*, 10191–10198; g) X.-P. Zhou, Z. Xu, M. Zeller, A. D. Hunter, S. S.-Y. Chui, C.-M. Che, J. Lin, *Inorg. Chem.* **2010**, *49*, 7629–7631; h) E. D. Bloch, D. Britt, C. Lee, C. J. Doonan, F. J. Uribe-Romo, H. Furukawa, J. R. Long, O. M. Yaghi, *J. Am. Chem. Soc.* **2010**, *132*, 14382–14384; i) A. D. Burrows, C. G. Frost, M. F. Mahon, C. Richardson, *Chem. Commun.* **2009**, 4218–4220; j) X.-P. Zhou, Z. Xu, M. Zeller, A. D. Hunter, S. S.-Y. Chui, C.-M. Che, *Inorg. Chem.* **2008**, *47*, 7459–7461.
- [5] a) S. Henke, R. A. Fischer, *J. Am. Chem. Soc.* **2011**, *133*, 2064–2067; b) Y.-H. Kiang, G. B. Gardner, S. Lee, Z. Xu, *J. Am. Chem. Soc.* **2000**, *122*, 6871–6883; c) Y.-H. Kiang, G. B. Gardner, S. Lee, Z. Xu, E. B. Lobkovsky, *J. Am. Chem. Soc.* **1999**, *121*, 8204–8215; d) M. Carbone, C. W. Abney, S. Liu, W. Lin, *Chem. Sci.* **2013**, *4*, 2396–2402.
- [6] a) Z. R. Herm, E. D. Bloch, J. R. Long, *Chem. Mater.* **2014**, *26*, 323–338; b) J.-R. Li, J. Sculley, H.-C. Zhou, *Chem. Rev.* **2012**, *112*, 869–932; c) Y. Liu, W. Xuan, Y. Cui, *Adv. Mater.* **2010**, *22*, 4112–4135; d) R. Ahmad, A. G. Wong-Foy, A. J. Matzger, *Langmuir* **2009**, *25*, 11977–11979; e) H. Wang, K. Yao, Z. Zhang, J. Jagiello, Q. Gong, Y. Han, J. Li, *Chem. Sci.* **2014**, *5*, 620–624.
- [7] a) L. E. Kreno, K. Leong, O. K. Farha, M. Allendorf, R. P. Van Duyne, J. T. Hupp, *Chem. Rev.* **2012**, *112*, 1105–1125; b) S. S. Nagarkar, B. Joarder, A. K. Chaudhari, S. Mukherjee, S. K. Ghosh, *Angew. Chem.* **2013**, *125*, 2953–2957; c) Y. Cui, H. Xu, Y. Yue, Z. Guo, J. Yu, Z. Chen, J. Gao, Y. Yang, G. Qian, B. Chen, *J. Am. Chem. Soc.* **2012**, *134*, 3979–3982; d) S. Pramanik, C. Zheng, X. Zhang, T. J. Emge, J. Li, *J. Am. Chem. Soc.* **2011**, *133*, 4153–4155.

- [8] a) A. Dhakshinamoorthy, M. Alvaro, H. Garcia, *Chem. Commun.* **2012**, 48, 11275–11288; b) X. Gu, Z.-H. Lu, H.-L. Jiang, T. Akita, Q. Xu, *J. Am. Chem. Soc.* **2011**, 133, 11822–11825; c) C. Wang, Z. Xie, K. E. de Krafft, W. Lin, *J. Am. Chem. Soc.* **2011**, 133, 13445–13454; d) D. T. Genna, A. G. Wong-Foy, A. J. Matzger, M. S. Sanford, *J. Am. Chem. Soc.* **2013**, 135, 10586–10589; e) L. Ma, C. Abney, W. Lin, *Chem. Soc. Rev.* **2009**, 38, 1248–1256.
- [9] a) B. Chen, S. Xiang, G. Qian, *Acc. Chem. Res.* **2010**, 43, 1115–1124; b) Y.-S. Bae, C. Y. Lee, K. C. Kim, O. K. Farha, P. Nickias, J. T. Hupp, S. T. Nguyen, R. Q. Snurr, *Angew. Chem. Int. Ed.* **2012**, 51, 1857–1860; *Angew. Chem.* **2012**, 124, 1893–1896; c) A. L. Dzubak, L.-C. Lin, J. Kim, J. A. Swisher, R. Poloni, S. N. Maximoff, B. Smit, L. Gagliardi, *Nat. Chem.* **2012**, 4, 810–816; d) D. Liu, H. Wu, S. Wang, Z. Xie, J. Li, W. Lin, *Chem. Sci.* **2012**, 3, 3032–3037; e) H. Wu, W. Zhou, T. Yildirim, *J. Am. Chem. Soc.* **2009**, 131, 4995–5000; f) S. Xiang, W. Zhou, J. M. Gallegos, Y. Liu, B. Chen, *J. Am. Chem. Soc.* **2009**, 131, 12415–12419; g) Q. Yang, C. Zhong, *J. Phys. Chem. B* **2006**, 110, 655–658; h) Y.-W. Li, J.-R. Li, L.-F. Wang, B.-Y. Zhou, Q. Chen, X.-H. Bu, *J. Mater. Chem. A* **2013**, 1, 495–499.
- [10] a) Y.-Q. Sun, C. Yang, Z. Xu, M. Zeller, A. D. Hunter, *Cryst. Growth Des.* **2009**, 9, 1663–1665; b) Y.-Q. Sun, J. He, Z. Xu, G. Huang, X.-P. Zhou, M. Zeller, A. D. Hunter, *Chem. Commun.* **2007**, 4779–4781.
- [11] a) Y.-Q. Lan, S.-L. Li, H.-L. Jiang, Q. Xu, *Chem. Eur. J.* **2012**, 18, 8076–8083; b) H. Kim, M. P. Suh, *Inorg. Chem.* **2005**, 44, 810–812; c) Z. Guo, R. Cao, X. Wang, H. Li, W. Yuan, G. Wang, H. Wu, J. Li, *J. Am. Chem. Soc.* **2009**, 131, 6894–6895.
- [12] a) A. Santra, I. Senkovska, S. Kaskel, P. K. Bharadwaj, *Inorg. Chem.* **2013**, 52, 7358–7366; b) C. Zhang, M. Zhang, L. Qin, H. Zheng, *Cryst. Growth Des.* **2014**, 14, 491–499; c) C. Zhang, H. Hao, Z. Shi, H. Zheng, *CrystEngComm* **2014**, 16, 5662–5671; d) L. Sarkisov, R. L. Martin, M. Haranczyk, B. Smit, *J. Am. Chem. Soc.* **2014**, 136, 2228–2231; e) Z. Wei, Z.-Y. Gu, R. K. Arvapally, Y.-P. Chen, R. N. McDougald, J. F. Ivy, A. A. Yakovenko, D. Feng, M. A. Omary, H.-C. Zhou, *J. Am. Chem. Soc.* **2014**, 136, 8269–8276.
- [13] Crystal data for BFMOF-1:  $C_{150}H_{125}N_3O_{30}Pb_6S_8$ ,  $M_r = 3949.30$ , crystal dimensions:  $0.240 \times 0.120 \times 0.080$  mm, triclinic, space group  $\bar{P}\bar{I}$  with  $a = 13.316(2)$  Å,  $b = 17.982(2)$  Å,  $c = 18.910(2)$  Å,  $\alpha = 116.429(2)^\circ$ ,  $\beta = 98.931(2)^\circ$ ,  $\gamma = 104.111(2)^\circ$ ,  $V = 3746.8(8)$  Å<sup>3</sup>,  $Z = 1$ ,  $\rho_{\text{calcd}} = 1.750$  g cm<sup>-3</sup>,  $\mu = 6.899$  cm<sup>-1</sup>,  $2\theta_{\text{max}} = 52.74^\circ$ , GOF = 1.034. A total of 48491 reflections were collected and 15282 are unique ( $R_{\text{int}} = 0.0354$ ).  $R_1(wR_2) = 0.0377$  (0.1012) for 997 parameters and 12896 reflections [ $I > 2\sigma(I)$ ]. The same framework structure can be crystallized using DMF (*N,N*-dimethylformamide) in place of DMA. CCDC-1020276 and 1020277 contain the supplementary crystallographic data for the two isoreticular structures of BFMOF-1 and BFMOF-1-DMF in this paper. These data can be obtained free of charge from The Cambridge Crystallographic Data Centre via www.ccdc.cam.ac.uk/data\_request/cif.
- [14] a) Z.-L. Xu, B. Liu, Q.-W. Wang, *Z. Kristallogr. New Cryst. Struct.* **2011**, 226, 515–517; b) M. R. St John Foreman, M. J. Plater, J. M. S. Skakle, *J. Chem. Soc. Dalton Trans.* **2001**, 1897–1903.
- [15] M. Zhang, Y.-P. Chen, M. Bosch, T. Gentle III, K. Wang, D. Feng, Z. U. Wang, H.-C. Zhou, *Angew. Chem. Int. Ed.* **2014**, 53, 815–818; *Angew. Chem.* **2014**, 126, 834–837.
- [16] Crystal data for BFMOF-1a:  $C_{138}H_{96}O_{26}Pb_6S_8$ ,  $M_r = 3669.76$ , crystal dimensions:  $0.327 \times 0.213 \times 0.101$  mm, triclinic, space group  $\bar{P}\bar{I}$ ,  $a = 13.079(4)$  Å,  $b = 15.531(5)$  Å,  $c = 17.946(6)$  Å,  $\alpha = 101.700(6)^\circ$ ,  $\beta = 106.280(7)^\circ$ ,  $\gamma = 100.948(6)^\circ$ ,  $V = 3306.5(2)$  Å<sup>3</sup>,  $Z = 1$ ,  $\rho_{\text{calcd}} = 1.843$  g cm<sup>-3</sup>,  $\mu = 7.807$  cm<sup>-1</sup>,  $2\theta_{\text{max}} = 50.70^\circ$ , GOF = 1.098. A total of 27434 reflections were collected and 12026 are unique ( $R_{\text{int}} = 0.0535$ ).  $R_1(wR_2) = 0.0521$  (0.1414) for 829 parameters and 7750 reflections [ $I > 2\sigma(I)$ ]. CCDC-1020278 contains the supplementary crystallographic data for BFMOF-1a in this paper. These data can be obtained free of charge from The Cambridge Crystallographic Data Centre via www.ccdc.cam.ac.uk/data\_request/cif.
- [17] a) X.-P. Zhou, Z. Xu, M. Zeller, A. D. Hunter, S. S.-Y. Chui, C.-M. Che, *Inorg. Chem.* **2011**, 50, 7142–7149; b) S. I. Swamy, J. Bacsá, J. T. A. Jones, K. C. Stylianou, A. Steiner, L. K. Ritchie, T. Hasell, J. A. Gould, A. Laybourn, Y. Z. Khimyak, D. J. Adams, M. J. Rosseinsky, A. I. Cooper, *J. Am. Chem. Soc.* **2010**, 132, 12773–12775; c) G. Huang, C. Yang, Z. Xu, H. Wu, J. Li, M. Zeller, A. D. Hunter, S. S.-Y. Chui, C.-M. Che, *Chem. Mater.* **2009**, 21, 541–546; d) P. D. Southon, L. Liu, E. A. Fellows, D. J. Price, G. J. Halder, K. W. Chapman, B. Moubaraki, K. S. Murray, J.-F. Létard, C. J. Kepert, *J. Am. Chem. Soc.* **2009**, 131, 10998–11009; e) J. Tian, P. K. Thallapally, S. J. Dalgarno, J. L. Atwood, *J. Am. Chem. Soc.* **2009**, 131, 13216–13217; f) D. Tanaka, S. Kitagawa, *Chem. Mater.* **2008**, 20, 922–931; g) Y. Zhang, B. Chen, F. R. Fronczeck, A. W. Maverick, *Inorg. Chem.* **2008**, 47, 4433–4435; h) M. Kawano, M. Fujita, *Coord. Chem. Rev.* **2007**, 251, 2592–2605; i) L. J. Barbour, *Chem. Commun.* **2006**, 1163–1168; j) L. Dobrzańska, G. O. Lloyd, H. G. Raubenheimer, L. J. Barbour, *J. Am. Chem. Soc.* **2006**, 128, 698–699; k) C. J. Kepert, *Chem. Commun.* **2006**, 695–700; l) J. L. Atwood, L. J. Barbour, A. Jerga, B. L. Schottel, *Science* **2002**, 298, 1000–1002.
- [18] G. Frenking, N. Froehlich, *Chem. Rev.* **2000**, 100, 717–774.
- [19] a) S. K. Bae, C. H. Heo, D. J. Choi, D. Sen, E.-H. Joe, B. R. Cho, H. M. Kim, *J. Am. Chem. Soc.* **2013**, 135, 9915–9923; b) N. Kumar, V. Bhalla, M. Kumar, *Coord. Chem. Rev.* **2013**, 257, 2335–2347; c) G.-J. Mao, T.-T. Wei, X.-X. Wang, S.-Y. Huan, D.-Q. Lu, J. Zhang, X.-B. Zhang, W. Tan, G.-L. Shen, R.-Q. Yu, *Anal. Chem.* **2013**, 85, 7875–7881; d) L. A. Montoya, T. F. Pearce, R. J. Hansen, L. N. Zakharov, M. D. Pluth, *J. Org. Chem.* **2013**, 78, 6550–6557; e) H. Zhang, P. Wang, G. Chen, H.-Y. Cheung, H. Sun, *Tetrahedron Lett.* **2013**, 54, 4826–4829; f) F. Zheng, M. Wen, F. Zeng, S. Wu, *Polymer* **2013**, 54, 5691–5697; g) L. A. Montoya, M. D. Pluth, *Chem. Commun.* **2012**, 48, 4767–4769; h) V. S. Lin, C. J. Chang, *Curr. Opin. Chem. Biol.* **2012**, 16, 595–601; i) H. Peng, W. Chen, Y. Cheng, L. Hakuna, R. Strongin, B. Wang, *Sensors* **2012**, 12, 15907–15946; j) A. R. Lippert, E. J. New, C. J. Chang, *J. Am. Chem. Soc.* **2011**, 133, 10078–10080.



J. Cui, Y.-L. Wong, M. Zeller, A. D. Hunter,  
Z. Xu\*

Pd Uptake and H<sub>2</sub>S Sensing by an  
Amphoteric Metal-Organic Framework  
with a Soft Core and Rigid Side Arms



**Yin and yang:** A system incorporating both rigid and flexible components has been prepared in which traditional configuration has been reversed by installing rigid side arms onto a soft core (see picture). After binding to Pb<sup>II</sup> ions, the dynamic hard–soft (carboxy–thioether) metal–organic framework has distinct amphoteric character, with the donor–acceptor properties enabling uptake of PdCl<sub>2</sub> and a sensitive colorimetric response to H<sub>2</sub>S.